Droplets movement and deposition of an eight-rotor agricultural UAV in downwash flow field

Tang Qing[1,2,3], Zhang Ruirui[1,2,3], Chen Liping[1,2,3*], Xu Min[1,2,3], Yi Tongchuan[1,2,3], Zhang Bin[1,2,3]

(1. *Beijing Research Center of Intelligent Equipment for Agriculture, Beijing Academy of Agriculture and Forestry Sciences, Beijing 100097, China*; 2. *National Research Center of Intelligent Equipment for Agriculture, Beijing 100097, China*; 3. *Beijing Key Laboratory of Intelligent Equipment Technology for Agriculture, Beijing 100097, China*)

Abstract: The movement and deposition of the droplets sprayed by agricultural unmanned aerial vehicle (UAV) are influenced by the complex downwash flow field of the rotors. Instead of conducting field experiment, a high speed particle image velocimetry (PIV) method was used to measure the movement and deposition of the droplets at different rotating speeds of rotors (1000-3000 r/min) or at different transverse injecting points (20-50 cm away from its nearby rotors) in the downwash flow field of an agricultural UAV with eight rotors and conical nozzles. The maximum speed and size of the high speed zone of the droplets were found greatly influenced by the downwash velocity. The initial spray angle of the nozzle declined with the increase of downwash flow speed. It was found that the downwash velocity could not only change the deposition zone of the droplets, but also influence their distribution. The increase of the downwash velocity would increase the deposition uniformity of the droplets. The nozzle position in the downwash flow field could also influence the deposition of the droplets. When the transverse distance between the nozzle and its nearby rotors increased, the relative deposition near the downwash flow of the rotors increased simultaneously. However, the distance between the deposition peak and the nozzle stayed constant. The initial spray angle of the nozzle was not influenced by the transverse distance between the nozzle and its nearby rotors. The research results could provide a theoretical basis and reference for the optimization of the spray application of multi-rotor UAV to minimize droplets deposition uncertainty.

Keywords: chemical spray, droplet deposition, UAV, flow field, multi-rotor

DOI: 10.3965/j.ijabe.20171003.3075

Citation: Tang Q, Zhang R R, Chen L P, Xu M, Yi T C, Zhang B. Droplets movement and deposition of an eight-rotor agricultural UAV in downwash flow field. Int J Agric & Biol Eng, 2017; 10(3): 47–56.

1 Introduction

At present, the rotor-powered micro and small agricultural unmanned aerial vehicles (UAV) developed rapidly in the plant protection, pollination and other agricultural areas[1-4]. The agricultural UAVs have a lot of prominent advantages such as low operating height, no need for special landing airport, flexible and lightweight, environmental adaptability and so on[5,6]. Its operating efficiency is about 30 times of the spray machine, and 100 times of manpower[7]. It can be applied to complex terrain environments such as hills, mountainous areas and

Received date: 2016-11-24 **Accepted date:** 2017-04-05

Biographies: Tang Qing, PhD, Assistant Professor, research interest: agricultural aerial spray, Email: tangq@nercita.org.cn; **Zhang Ruirui**, PhD, Associate Professor, research interest: agricultural sensor network, Email: zhangrr@nercita.org.cn; **Xu Min**, PhD, associate professor, research interests: flight control and navigation, Email: xum@nercita.org.cn; **Yi Tongchuan**, Assistant Engineer, research interests: electrics and electronics, Email: yitc@nercita.org.cn; **Zhang Bin**, PhD candidate, research interest: computational fluid dynamics, Email: zhangbinastro@mail.nwpu.edu.cn.

***Corresponding author: Chen Liping**, PhD, Professor, research interests: intelligent agricultural technology, precision agriculture. National Research Center of Intelligent Equipment for Agriculture, No.11 Shuguang Huayuan Middle Road, Haidian District, Beijing 100097, China. Tel/Fax: +86-10-51503425, Email: chenlp@nercita.org.cn.

sloping fields for rice pollination and high-stem crop protection, where the ground agricultural machinery is very difficult to carry out work[5].

Influenced by the downwash flow of the rotor, the movement and deposition law of sprayed droplets are distinctly different from that of traditional spraying instruments[8]. The coverage width of the wind field, the wind speed in the wind field and the distribution law of the wind field will directly affect the movement and deposition of the droplet[9].

There have been a lot of achievements on field research of UAVs, especially on the research of actual operation conditions. Zhang et al.[6] used polyethylene plastic wire to collect the droplets sprayed by the unmanned helicopter, and optimized the UAV operation height and speed. Kang et al.[10] reported aerial spray results of a conventional unmanned agricultural helicopter, and showed 20% greater deposition on the right side. Qin et al.[11,12] used the polyester card in the corn canopy to collect droplets at different heights, and studied the unmanned helicopter spray parameters on the corn canopy droplet deposition distribution. Bae et al.[13] developed an unmanned roll-balanced helicopter and tested its spray deposition distribution by using a string deposition analysis system. Zhang et al.[14] evaluated the spray effect of a quad-rotor UAV in citrus orchard with different operating heights and nozzle types.

A number of studies focused on the effects of the downwash flow field of UAVs. Giles et al.[15,16] used metallic tracers to quantify the spray deposition of an unmanned helicopter for crop spraying. Wang et al.[17] used the wind field wireless sensor network measurement system to test the wind field of an unmanned helicopter. The results suggest that the Z3 model helicopter's best flight operation height is 7 m, and the headwind flight should be avoided. Li et al.[18] also used the wind field wireless sensor network measurement system to measure the wind field distribution of a multi-rotor UAV. However, the field measurement of the rotor downwash flow field still suffers from low spatial and temporal resolution, since a lot of high precision measuring instruments are not applicable in field measurement. At the same time, the turbulence of the atmospheric boundary layer can reach 10% to 15%[19], which will also greatly affect the repeatability of field experiment results.

The basic research about the downwash flow field generated by a rotor was reported much earlier. As early as in 1952, Gessow et al.[20] completed the monograph on helicopter aerodynamics. To 1986, Gessow et al.[21] and Johnson et al.[22] reviewed the aerodynamic about the helicopter and rotor respectively. Focused on experimental measurements, Raffel et al.[23] summarized the evaluation of rotor flow using particle image velocimetry (PIV) techniques, and indicated that PIV method could form a basis of a vortex development and aging model for the blade tip vortices. Wall et al.[24] used two dimensional and three components (2D-3C) PIV technique to analyze the rotor speed field data. Johnson et al.[25] used high-speed PIV to study the transport of ground sediments resulting from rotor rotation. Particles reaching sufficient heights were observed to recirculate into the rotor wake, and convect back towards the ground. Nathan et al.[26] used the PIV technique to measure the rotor flow field including the ground effect, and found that under different flight attitude, the flow state changed greatly. Conlisk et al.[27] wrote a review about the flow structures generated by the rotors. Many sophisticated experimental and computational techniques have been employed in an effort to predict performance parameters. But the current researches mainly focus on the micro-mechanism of the downwash flow field. There still are few researches focusing on the movement and deposition of the droplets in the downwash flow field of a multi-rotor UAV.

In this research, an 8-rotor agricultural UAV was fixed on a bracket to form a stable and controllable downwash flow field in the laboratory. A high-speed PIV system was used to directly record the spatial distribution of droplets sprayed by the nozzle. Based on the time-dependent velocity field algorithm and the spatial particle image superposition algorithm, the high precision droplet velocity distribution and the droplet spatial density distribution image could be obtained respectively. The results of the experiment show that the rotating speed of the rotor and the nozzle position could both influence the movement and deposition of the

droplets in the downwash flow field of the multi-rotor UAV.

2 Materials and methods

2.1 UAV system

The UAV (model: TTA M8A, Tian Tu Aviation) tested in this study was fixed by four aluminum alloy supports, as shown in Figure 1. The height from the rotor to the ground is about 2 m.

Figure 1 The 8-rotor UAV with spraying devices and PIV system

The detailed parameters of the UAV are listed in Table 1.

Table 1 Parameters of the TTA M8A UAV

Parameters	Technical index
Rotor base/m	1.46
Operating speed/m·s^{-1}	0-15
Spray swath/m	4-5
Load/kg	10
Operating duration/min	10-15
Operating temperature/°C	–25 to 50
Operating height/m	1-3

2.2 Spray system

The original spray system of the UAV was used to generate droplets with volume mean diameter $Dv_{0.5}$= 100 μm through the TR-80-005c nozzle, which is made by Lechler Co., Ltd. As shown in Figure 2, the nozzle was mounted on a spray beam which is 20 cm below the rotors, with different spanwise distribution (x=20 mm, 30 mm, 40 mm, 50 mm).

2.3 Time-resolved PIV (TR-PIV) systems

Because the self- and mutually-induced effects on helicoidal could wake vortices, the flow induced by rotors is aperiodic[28]. Therefore, time-resolved PIV (TR-PIV) measurements were chosen to measure the flow field. TR-PIV allows the proper temporal evolution of the flow to be examined, albeit with somewhat reduced spatial resolution[25]. The present TR-PIV system incorporated a high-speed digital camera with a double-pulsed Nd:YLF (a kind of laser crystal with chemical formula: $LiY_{1.0-x}Nd_xF_4$) laser. This combination allowed temporal velocity measurements to be made at a rate up to 1000 Hz with full pixel (1024×1280) resolution. Although the advantages of the TR-PIV system are obvious, the extremely high repetition rate of the Nd:YLF laser results in a much lower light energy per pulse. However, we just focused on the movement of the droplets generated by the nozzles, which were much larger than the tracer particles usually used in PIV. Thus, there was no illumination challenge for the experiment. The schematic diagram of the experiment is shown in Figure 2.

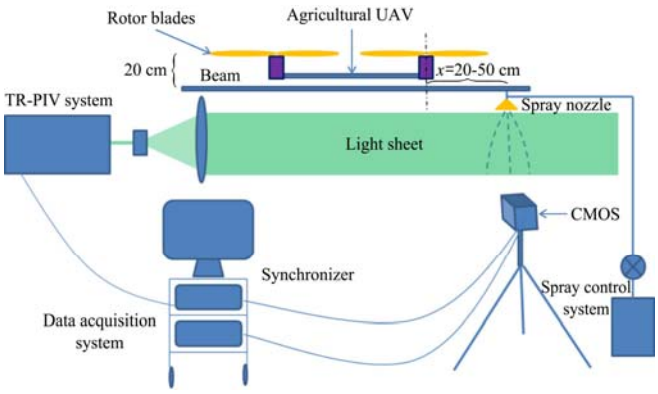

Figure 2 Schematic diagram of the experiment

In the present experiment, a total of 1000 sequential images were taken for each data set by using a high speed CMOS. The illumination of the light sheet was enhanced by a convex lens and the illuminating area was 500 mm × 500 mm (length (Y) × width (X)).

3 Results and discussion

3.1 Effects of downwash flow to the movement and deposition of the droplets

Firstly, we tried to study the effects of rotors rotating speed to the droplets movement and deposition. The spray pressure was 0.2 MPa and the flow rate was 1.25 L/min. The rotating speed of the rotors was set to 0, 1000 r/min, 2000 r/min and 3000 r/min.

Figure 3 shows the droplets photographed at different rotating speeds. The nozzle orifice was at 147 mm position and the rotor was at 47 mm position in x-direction in the photograph, shown by the red arrow.

In Figure 3a, we could see that without downwash flow, the total spray angle of the nozzle was about 76°. The droplets assembled and moved turbulently in the inner spray area (33° around the centerline), and atomized and moved smoothly in the outer spray area. Figure 3b shows that the initial spray angle of the nozzle and the droplets in the outer area were stable at the downwash flow field. However, the droplets in the inner area moved obviously off the centerline to the direction of rotors. In Figure 3c, the initial spray angle of the nozzle declined slightly. The deviation of the droplets to the centerline became larger and the outer area under the rotors was also become unstable. In Figure 3d, we could see that the initial spray angle of the nozzle became even smaller due to the large downwash flow. The deviation of the droplets to the centerline was not too large and the droplets in the outer area were still stable. In general, the spray angle of the nozzle declined with the increase of the downwash flow speed, and the droplets in the inner spray area were greatly affected by the downwash flowed and inclined to the direction of rotors.

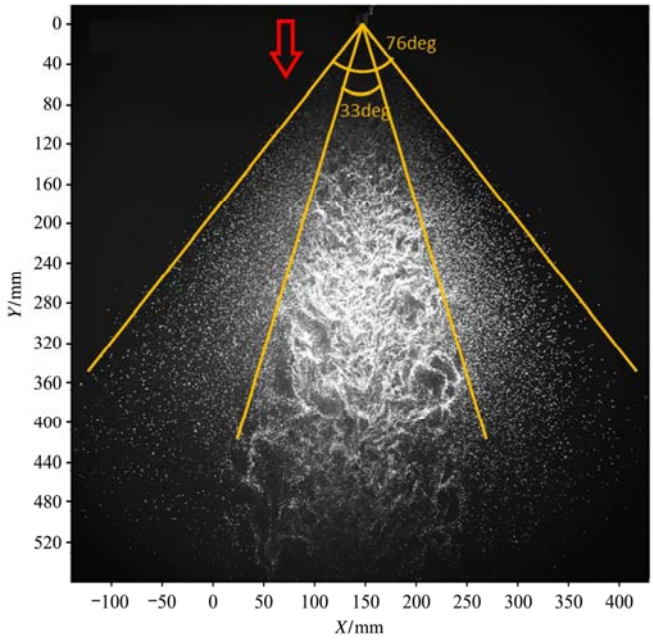

a. 0

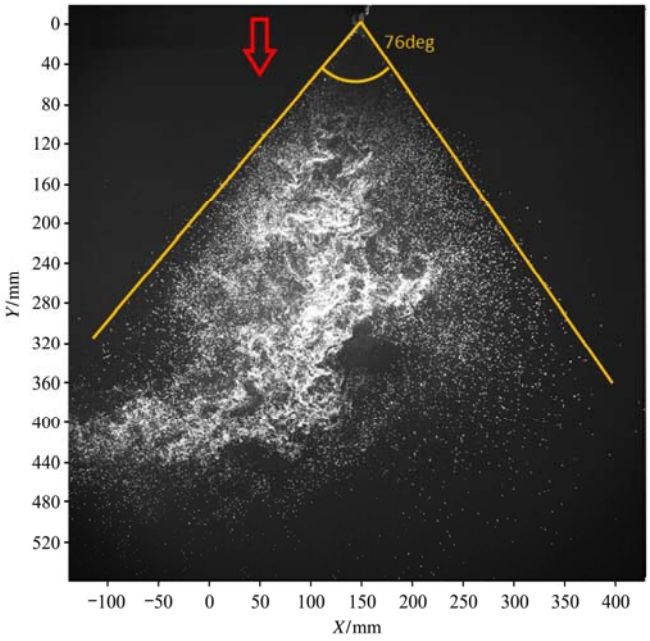

b. 1000 r/min

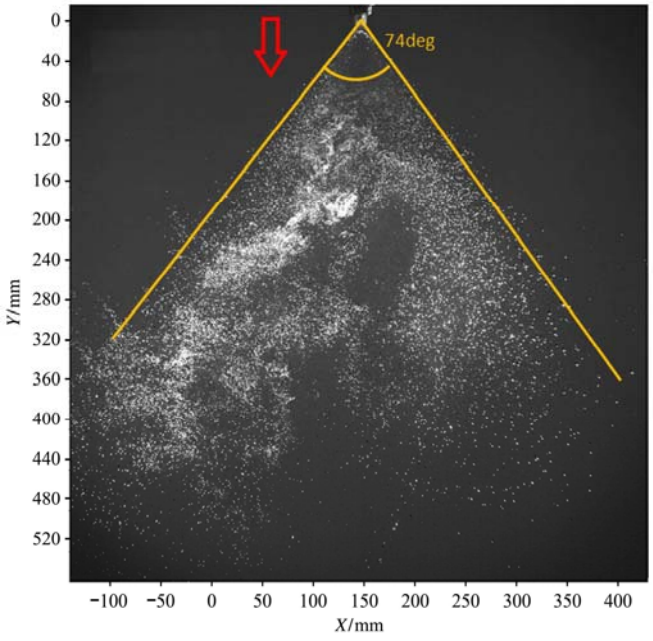

c. 2000 r/min

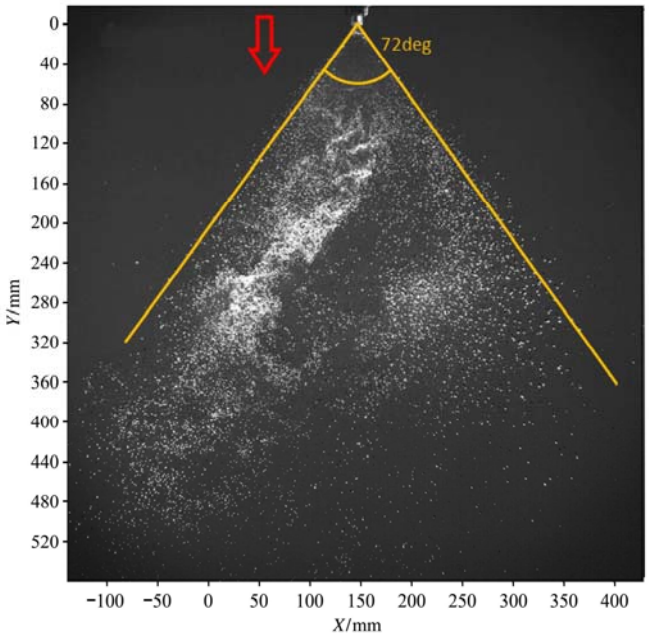

d. 3000 r/min

Figure 3 Pictures of the instantaneous droplets at different downwash flow speeds

Figure 4 shows the averaged velocity field of the droplets at different rotating speed. One thousand contiguous instantaneous fluid velocity vector maps were used to obtain the local time-averaged fluid velocities. The resolution of the images is 1024×1280 pixels and the correlation window size is 128×128 pixels. The edge of the effective area of the relatively higher speed was lined out by black lines. The nozzle orifice is shown by the black arrow, and the rotor's downwash flow in *x*-direction is shown by the red arrow.

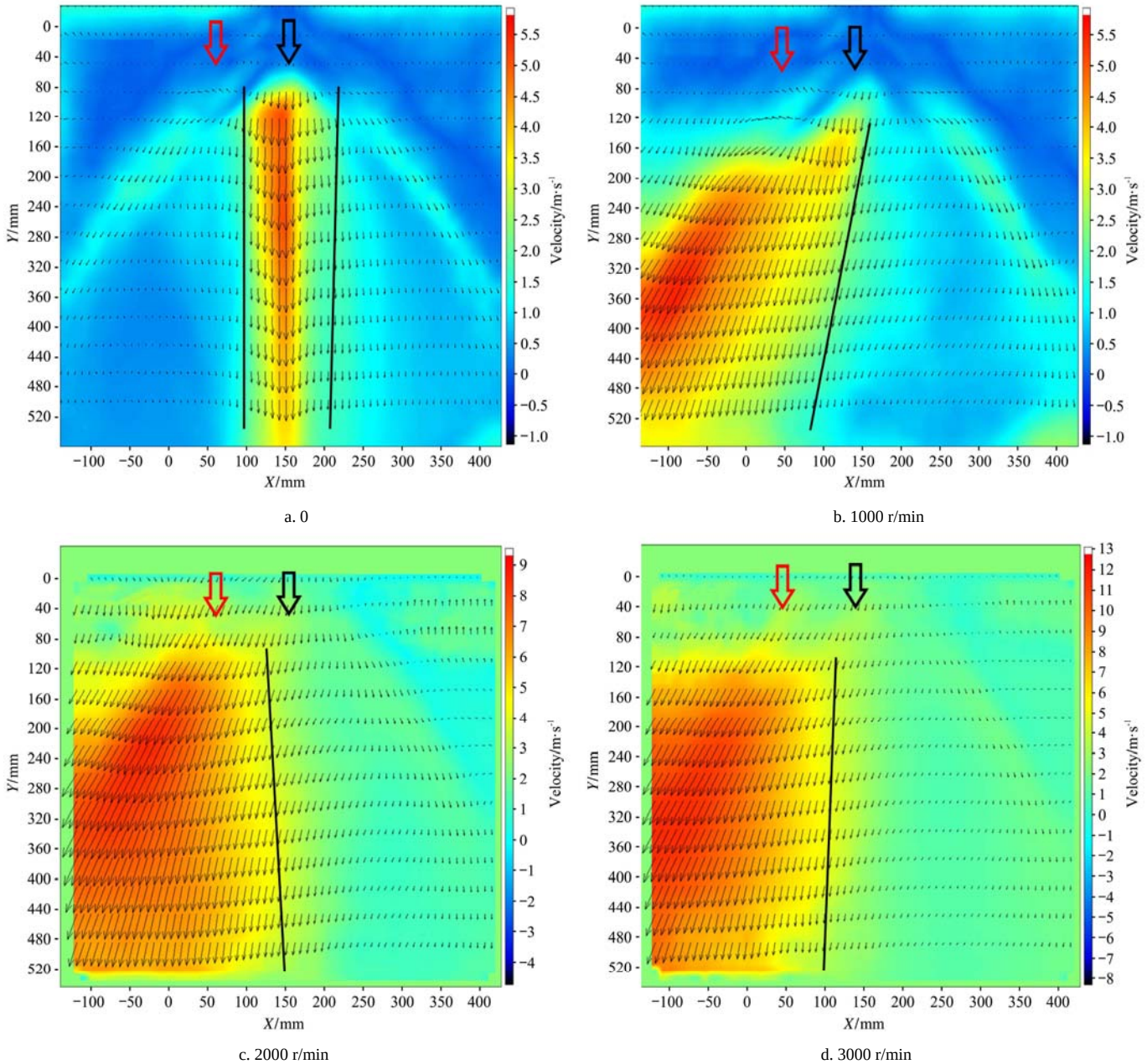

a. 0 b. 1000 r/min

c. 2000 r/min d. 3000 r/min

Figure 4 Averaged droplet velocity fields at different downwash flow speeds

Figure 4a shows that the maximum speed of the droplets was less than 5.5 m/s and appeared near the centerline. The effective width of the high speed zone is about 100 mm. The speed in outer area away from the centerline is about 1-1.5 m/s, vertical to the ground. The droplets' speed near the spray edge is about 1.5 m/s, parallel to the generatrix of the spray cone.

Figure 4b shows that the high speed zones inclined to the downwash flow field under the rotors. The maximum speed of the droplets was about 5.5 m/s, while the effective width of the high speed zone is more than 300 mm, which is much larger than that in Figure 4a. The droplet movement direction of the spray also slightly inclined to the downwash flow area.

In Figure 4c, the high speed zone coverage of the droplets (in x<150 mm zone) became larger. The

movement speed of the droplets was up to 8 m/s at the high speed area. The droplet speed at the low speed zone was about 2 m/s, with the direction inclined to the downwash flow field.

Figure 4d shows that the maximum movement speed of the droplets in the high speed zone was up to 12 m/s, the right edge of which was at x=100 mm.

Based on the droplets images, we can also estimate the deposition of droplets at 400 mm under the nozzle. One thousand images of the droplets were processed to remove the non-uniform background. The grey scale profile at 400 mm under the nozzle was taken, which could partly indicate the spatial density distribution of the droplets.

Figure 5 shows the grey scale distribution normalized by the maximum value on the profile, and we used 0.5 as a critical value to calculate the deposition width of the droplets.

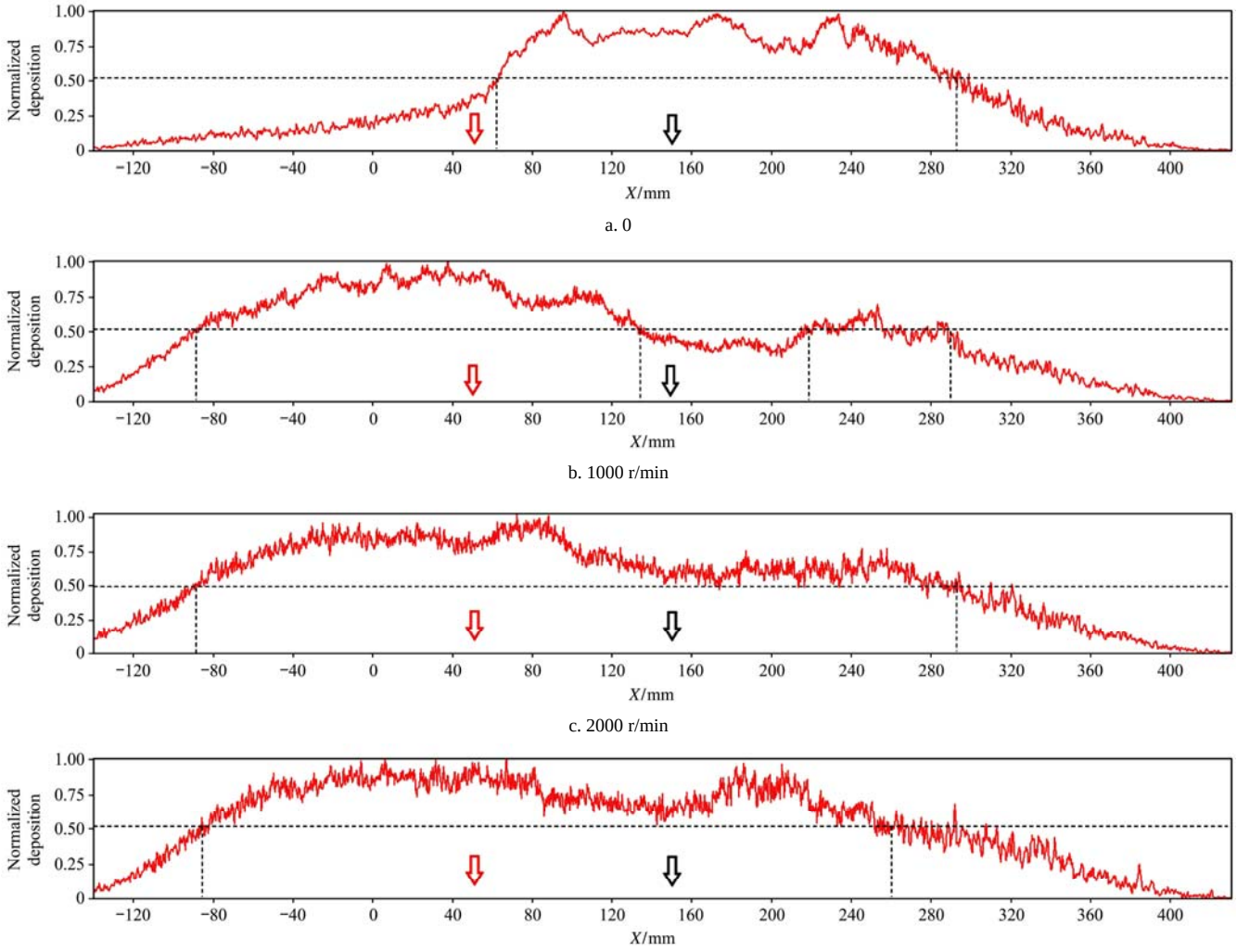

a. 0

b. 1000 r/min

c. 2000 r/min

d. 3000 r/min

Figure 5 Spatial distribution of the droplets at zone 400 mm under the nozzle at different downwash flow speeds

From Figure 5a, we could see that the deposition width of the droplets is about 230 mm, with a quasi-unimodal distribution.

Figure 5b shows the deposition of the droplets with a double peak structure. The width of the main peak is about 220 mm and the width of the second peak is about 70 mm.

Figure 5c shows that the deposition width of the droplets is about 380 mm. The double peak structure in the figure is not so clear. The main peak is under the downwash flow of the rotor, and the second peak is on the right of the nozzle orifice, which is flat and about half of the height of the main peak.

Figure 5d shows a narrower deposition zone of the droplets than Figure 5c, which has a width about 350 mm. The second peak in the right of the nozzle orifice is higher than Figure 5c.

Generally, downwash flow would increase the

deposition area of the droplets for about 150%, and the main peak of the deposition of droplets is approach to the downwash flow zone. The increase of rotors rotation rate will make the deposition more uniform.

3.2 Effect of droplets' injecting point on their movement and deposition

Secondly, we tried to study the effect of the droplets' injecting point on their movement and deposition. We moved the nozzle away from the rotors transversely, and the nozzle position was x=20 cm, 30 cm, 40 cm, 50 cm in turn.

The droplets' distribution in the space of each case mentioned above is shown in Figure 6. The position of the rotor (downwash flow direction) is shown by the red arrow.

From Figure 6, it can be seen that although the nozzle was placed away from the rotors along x-direction, the droplets were still affected by the downwash flow field of the rotors. The turbulent flow near the centerline of the spray nozzle was attracted by the downwash flow, and moved out of the spray range occasionally. However, the spray angle of the nozzle seems was not quite influenced by its position in the downwash flow field.

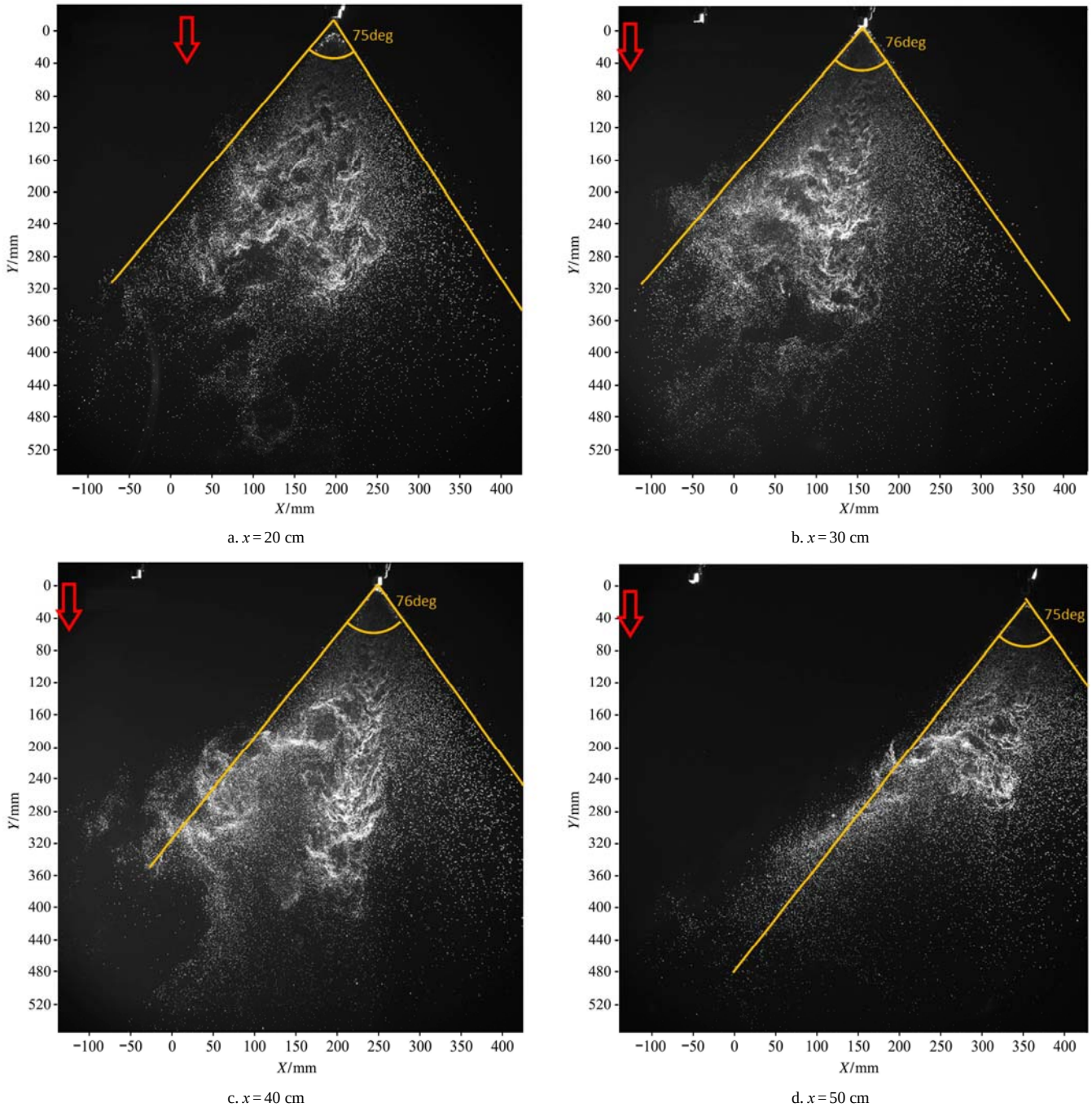

a. x = 20 cm

b. x = 30 cm

c. x = 40 cm

d. x = 50 cm

Figure 6 Pictures of the instantaneous droplets at different transverse nozzle positions

The movement of the droplets generated by the nozzle at different transverse positions is shown in Figure 7. The red arrow indicates the direction of the downwash flow of the rotor and the black arrow indicates the position of the nozzle orifice.

Figures 7a and 7b show that the high speed zone of the droplets distributes as a one peak structure, which inclines to the direction of the downwash flow.

Figures 7c and 7d show that when the distance between the nozzle orifice and the downwash flow is more than 40 cm, the structure of the droplet movement changes from one peak to double peaks. When the distance exceeds 50 cm, the second peak of the flow speed becomes very weak.

The moving direction of the droplets away from the downwash flow will be changed by the attraction effect. As shown in Figures 7a-7c, the moving trace of the droplets on the right side curves to the left.

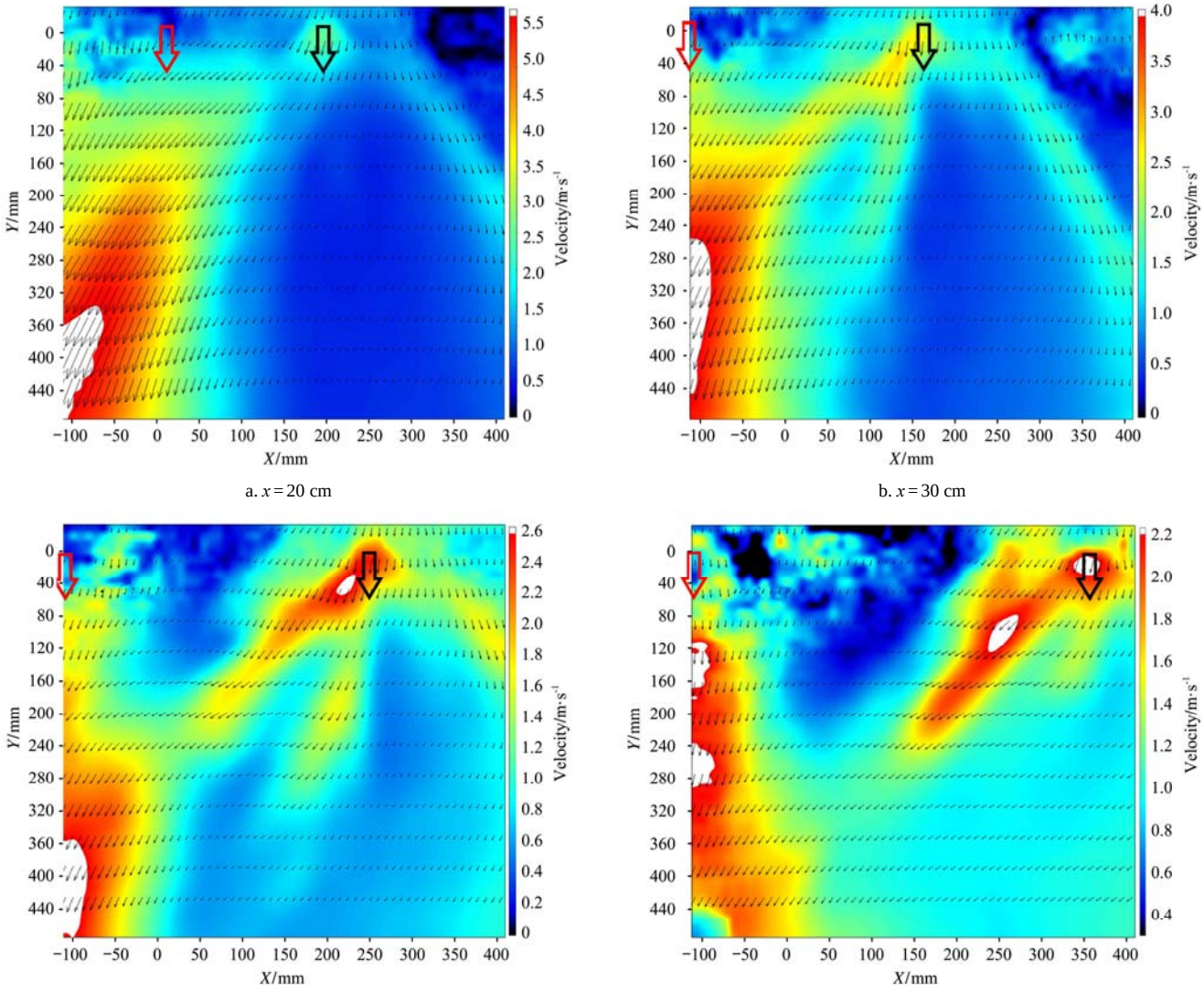

a. x = 20 cm b. x = 30 cm

c. x = 40 cm d. x = 50 cm

Figure 7 Averaged velocity fields of the droplets generated by nozzle at different transverse positions

The deposition of the droplets is also influenced by the transverse position of the nozzle, which is shown in Figure 8.

From Figure 8a, we could see that the deposition width of the droplets is about 270 mm, with a quasi-unimodal distribution.

Figure 8b shows a deposition of the droplets with a double peak structure. The width of the deposition area of the two peaks is about 270 mm and the width of the main peak is 190 mm. The small peak is near the downwash flow and the height of the peak is about 0.6 times of the main peak near the nozzle.

Figure 8c shows that the deposition width of the droplets is about 290 mm. The double peak structure in the figure is very clear. The sizes of the two peaks are similar and the whole deposition area is near the nozzle.

Figure 8d shows a deposition of the droplets with a double peak structure. The small peak is near the downwash flow and the height of the peak is about 0.5 times of the main peak near the downwash flow. The width of the main peak is about 120 mm.

Generally, the downwash flow generated a low pressure zone which could attract droplets moving toward it. When the distance between the nozzle and the downwash flow is increased, the deposition peak near the downwash flow grows simultaneously. However, the distance between the left deposition peak and the nozzle stays constant, as shown by the red dashed line in Figure 8.

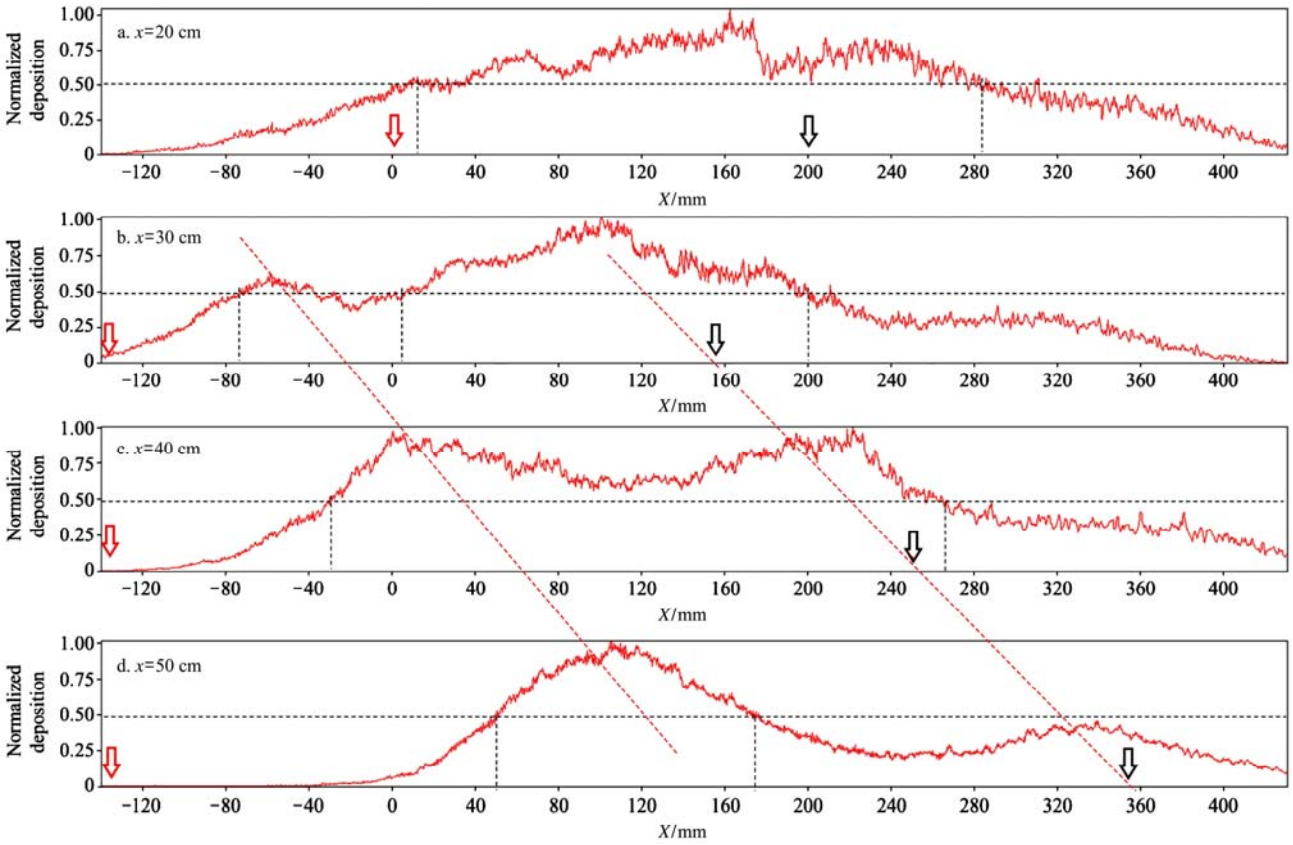

Figure 8 Spatial distribution of the droplets at different nozzle transverse positions (400 mm positions under the nozzle)

4 Conclusions

A high speed PIV method was used to measure the movement and deposition of the droplets at different rotating speeds of the rotors or at different transverse injecting points in the downwash flow field of an agricultural UAV with eight rotors and conical nozzles. The main findings of the experiment are summarized below:

1) The initial spray speed of the droplets generated by the nozzle was less than 5 m/s, while the speed of the droplets in the downwash flow could be up to 12 m/s. This indicated that the movement of the droplets is mainly affected by the downwash flow.

2) The increase of the downwash flow speed would decline the spray angle of the nozzle for about 5%, when the nozzle was in the effective zone of the downwash flow and the spray direction was the same as the flow.

3) The downwash flow could broaden the droplet deposition area for about 150%. The increase of the rotating speed of rotors could make the droplet deposition more uniform.

4) The distance between the nozzle and the downwash flow could influence the deposition of the droplets. When the distance between the nozzle and the downwash flow was increased, the deposition peak near the downwash flow grew simultaneously. However, the spray angle of the nozzle, and the distance between the deposition peak and the nozzle, stayed constant.

Acknowledgements

This work was supported by the National Natural Science Foundation of China (31601228), the Youth Science Fund of the Beijing Natural Science Foundation

(6164032), the Youth Science Fund of Beijing Academy of Agriculture and Forestry Sciences (QNJJ201631), and Zhang Ruirui's Beijing Talent Program.

[References]

[1] Zhang D Y, Lan Y B, Chen L P, Wang X, Liang D. Current status and future trends of agricultural aerial spraying technology in China. Transactions of the CSAM, 2014; 45(10): 53–59. (in Chinese)

[2] Swain K C, Thomson S J, Jayasuriya H P W. Adoption of an unmanned helicopter for low-altitude remote sensing to estimate yield and total biomass of a rice crop. Transactions of the ASABE, 2010; 53(1): 21–27.

[3] Swain K C A, Jayasuriya H P W, Salokhe V M. Suitability of low-altitude remote sensing images for estimating nitrogen treatment variations in rice cropping for precision agriculture adoption. Journal of Applied Remote Sensing, 2007; 1(1): 6656–6659.

[4] Huang Y B, Hoffmann W C, Lan Y B, Wu W F, Fritz B K. Development of a spray system for an unmanned aerial vehicle platform. Applied Engineering in Agriculture, 2009; 25(6): 803–809.

[5] Kirk I W, Hoffmann W C, Fritz B K. Aerial application methods for increasing spray deposition on wheat heads. Applied Engineering in Agriculture, 2007; 23(6): 357–364.

[6] Zhang J, He X K, Song J L, Zeng A J, Liu Y J, Li X F. Influence of spraying parameters of unmanned aircraft on droplets deposition. Transactions of the CSAM, 2012; 43(12): 94–96. (in Chinese)

[7] Zhou Z Y, Zang Y, Luo X W, Lan Y B, Xue X Y. Technology innovation development strategy on agricultural aviation industry for plant protection in China. Transactions of the CSAE, 2013; 29(24): 1–10. (in Chinese)

[8] Ramasamy M, Lee T E, Leishman J G. Flow field of a rotating-wing micro air vehicle. Journal of Aircraft, 2012; 44: 1236–1244.

[9] Wang L, Lan Y B, Hoffmann W C, Fritz B K, Chen D, Wang S M. Design of variable spraying system and influencing factors on droplets deposition of small UAV. Transactions of the CSAM, 2016; 47(1): 15–22. (in Chinese)

[10] Kang T G, Lee C S, Choi D K, Jun H J, Koo Y M, Kang T H. Development of Aerial Application System Attachable to Unmanned Helicopter: Basic Spraying Characteristics for Aerial Application System. Journal of Biosystems Engineering, 2010; 35(4): 215–223.

[11] Qin W C, Xue X Y, Zhou L X, Zhang S C, Sun Z, Kong W, et al. Effects of spraying parameters of unmanned aerial vehicle on droplets deposition distribution of maize canopies. Transactions of the CSAE, 2014; 30(5): 50–56. (in Chinese)

[12] Qin W C, Qiu B J, Xue X Y, Chen C, Xu Z, Zhou Q Q. Droplet deposition and control effect of insecticides sprayed with an unmanned aerial vehicle against plant hopper. Crop Protection, 2016; 85: 79–88.

[13] Bae Y, Koo Y M. Flight attitudes and spray patterns of a roll-balanced agricultural unmanned helicopter. Applied Engineering in Agriculture, 2013; 29(5): 675–682.

[14] Zhang P, Lyu Q, Yi S L, Liu Y, He S L, Xue R J, et al. Evaluation of spraying effect using small unmanned aerial vehicle (UAV) in citrus orchard. Journal of Fruit Science, 2016; 33(1): 34–42.

[15] Giles D K, Billing R, Anderson P G, Balsari P, Carpenter P I, Cooper S E, et al. Unmanned aerial platforms for spraying: deployment and performance. Aspects of Applied Biology, 2014; 12: 63–69.

[16] Giles D K, Billing R. Deployment and Performance of a UAV for Crop Spraying. Chemical Engineering Transactions, 2015; 44: 307–312.

[17] Wang P, Hu L, Zhou Z Y, Yang W S, Liu A M, Luo X W, et al. Wind field measurement for supplementary pollination in hybrid rice breeding using unmanned gasoline engine single-rotor helicopter. Transactions of the CSAE, 2013; 29(3): 54–61. (in Chinese)

[18] Li J Y, Zhou Z Y, Hu L, Zang Y, Xu S, Liu A M, et al. Optimization of operation parameters for supplementary pollination in hybrid rice breeding using uniaxial single-rotor electric unmanned helicopter. Transactions of the CSAE, 2014; 30(10): 10–17. (in Chinese)

[19] Garratt J R. The atmospheric boundary layer. Cambridge University Press, 1992.

[20] Gessow A, Myers G. Aerodynamics of the helicopter. NewYork: Macmillan Company, 1952.

[21] Gessow A. Understanding and predicting helicopter behavior then and now. Journal of the American Helicopter Society, 1986; 31(1): 3–28.

[22] Johnson W. Recent developments in rotary-wing aerodynamic theory. AIAA Journal, 2015; 24(8): 1219–1244.

[23] Raffel M, Richard H, Ehrenfried K, Wall B G, Burley C. Recording and evaluation methods of PIV investigations on a helicopter rotor model. Experiments in Fluids, 2004; 36(1): 146–156.

[24] Wall B G, Richard H. Analysis methodology for 3C-PIV data of rotary wing vortices. Experiments in Fluids, 2006; 40(5): 798–812.

[25] Johnson B, Leishman J G, Sydney A. Investigation of sediment entrainment using dual-phase, high-speed particle image velocimetry. Journal of the American Helicopter Society, 2010; 55(4): 042003.

[26] Nathan N D, Green R B. The flow around a model helicopter main rotor in ground effect. Experiments in Fluids, 2012; 52: 151–166.

[27] Conlisk A T. Modern helicopter aerodynamics, Ann. Rev. Fluid Mech. 1997; 21: 515–567.

[28] Mccroskey W. Vortex wakes of rotorcraft. 33rd Aerospace Sciences Meeting and Exhibit Reno, NV, USA. 1995; 95–0530.